Estimating Contact Forces from Postural Measures in a class of Under-Actuated Robotic Hands

Cosimo Della Santina[1], Cristina Piazza[1], Gaspare Santaera[2], Giorgio Grioli[2], Manuel Catalano[2], and Antonio Bicchi[1]

***Abstract*— Sensing contact forces can be a key enabler for higher order dexterous manipulation in robotic hands. To sense the full range of contact pressure distribution would provide the best solution, but it is in practice unfeasible when considering very deformable and adaptable hands. This paper proposes an approach to estimate the contact forces acting on an under-actuated adaptable hand by combining the compliance model of the hand with the geometric configuration of the hand itself. This is done by introducing reasonable assumptions about the net contact force on each phalanx. The proposed method is introduced and experimentally validated on two fingers of the Pisa/IIT SoftHand.**

I. INTRODUCTION

Over the years, several hand designs were proposed to try to match the level of dexterity of the human hand. Among them soft hands are getting increasing interest [1] [2] [3]. With the term soft hand we refer to a class of under-actuated hands presenting a soft behavior, as a result of the embedding of elastic elements with either fixed or variable mechanical characteristics [4], combined with the use of under-actuation [5]. Among them the Pisa/IIT SoftHand [6] and its evolutions [7] [8] are soft hands implementing the concept of soft synergies [9]. In this model the reference posture for the hand is generated as a combination of a reduced set of basic movements, called synergies [10]. The physical hand is attracted towards the reference posture by forces which are generated by the internal hand impedance, but it is also repelled by interaction forces generated by the contact with the environment. The actual hand posture naturally results as the equilibrium between these two actions.

Thanks to their intrinsic compliance, soft hands enable new paradigms in planning and control of grasping, moving from the timid approach of traditional rigid and fragile hands, to a more daring one [11]. In [12] it is discussed how humans are able to exploit objects and environmental constraints to functionally shape their hands. Analogously soft hands are mechanically able to go beyond their nominal kinematic limits by exploiting their structural softness. Furthermore in [6] it is shown that is possible to perform effective grasps with just a rough knowledge of the object to be grasped and of the environment. This diverts strongly from traditional grasping strategies designed for rigid fully actuated hands.

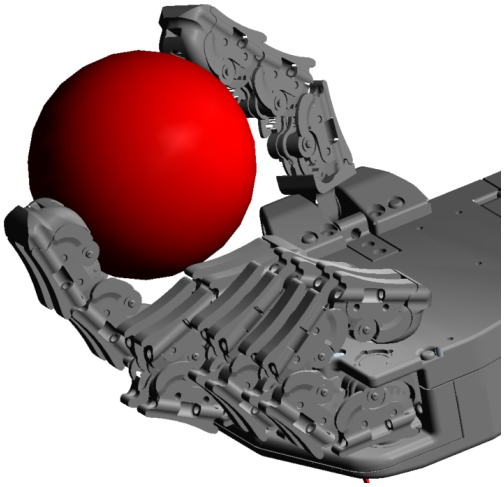

Fig. 1. An under-actuated soft hand grasping an object. Finger with a contact force applied on close much less than fingers not in contact with the object. Thus by looking to the hand posture is possible to infer which fingers are in contact and which are not. This is the simple intuition that motivates the present approach.

Soft hands are also interesting because they require and promote novel approaches in sensing. Conforming naturally to the environment, information coming from the hand state can be used to infer information about the environment itself and about the nature of the interaction. In [13] the geometry of an object grasped with a soft gripper is estimated from the gripper configuration, while in [14] the hand displacement is used to infer the location of an incidental collision. More recently in [15] authors consider the problem of deriving tactile data solely from proprioceptive sensors attached to the actuator of an under-actuated finger.

In this work we face the problem of estimating contact forces in a class of under-actuated hands which includes those whose design is based on soft synergies [6]. In the state of the art, a lot of effort was devoted to the design of sophisticated solutions for force sensing, successfully used with many robotic hands. However such solutions tend to be expensive and bulky [16]. Other studies face the problem of deriving force information from other sources. Examples are [17] and [18] where forces are estimated from vision, and [19] where the presence of an impact is estimated from kinematic measures.

*This work was supported by the European Commission projects (Horizon 2020 research program) SOFTPRO (no. 688857) and SOMA (no. 645599) and by the European Research Council under the Advanced Grant SoftHands "A Theory of Soft Synergies for a New Generation of Artificial Hands" (no. ERC-291166)

[1]Centro di Ricerca "E. Piaggio", Universita di Pisa, Largo L. Lazzarino, 1, 56126 Pisa, Italy.

[2]Department of Advanced Robotics, Istituto Italiano di Tecnologia, Genoa, Italy

Correspond to: cosimodellasantina at gmail.com

We propose here a method to estimate contact forces just by sensing static posture measures. The underling idea of the method is to consider the differences between actual posture and the reference hand posture. From that information, contacts and interaction forces are estimated relying on the knowledge of hand compliance. Fig. 1 suggests the intuition behind our approach: for a given command on the hand actuator the thumb and index do not close as much as the other fingers because of the contact forces. The performance of the proposed method is still to be fully tested, and the authors do not expect to reach the levels of accuracy typically achieved by traditional and commercial grade sensors. Nevertheless we believe that this technology is still promising for a set of applications that range from low-cost systems, to grasp acquisition acknowledgment.

The paper is organized as follows in section II the problem is defined and in section III a naive solution is shown to be ineffective. In section IV the estimator is introduced and in section V its theoretical performance is tested in simulations. Section VI defines the details of the application of our method to the kinematics of the Pisa/IIT SoftHand fingers and finally in section VII experimental results are provided, supporting the effectiveness of the method.

II. PROBLEM STATEMENT

A broad class of robotic hands, characterized by under-actuated mechanisms and comprising elastic return elements, can be described [20] by the system

$$\begin{cases} Rq = x & (1) \\ J^T f_{\text{ext}} = R^T f - E(q)\,, & (2) \end{cases}$$

where $q \in \mathbb{R}^n$ is the vector of the Lagrangian joint coordinates, $x \in \mathbb{R}^s$ is the vector of the generalized actuators displacements[1], $R \in \mathbb{R}^{s\times n}$ is the transmission matrix, that maps displacements of the joints in displacements of the actuators, $f \in \mathbb{R}^s$ is the vector of the generalized actuator forces, $f_{\text{ext}} \in \mathbb{R}^M$ is the vector that collects all the wrenches acting the various contact points[2], while $J \in \mathbb{R}^{M\times n}$ is the matrix formed by the juxtaposition of all the Jacobians in each contact point $J_i(q)$ as in

$$J^T = \left[J_1^T, J_2^T, \cdots\right]\,. \tag{3}$$

An illustration of the previous equations is shown in Fig. 2.

This paper considers the problem of reconstructing the set of the contact wrenches acting on the hand based on the sole knowledge of the robot hand model, its joints configurations q, and its actuators generalized forces f. With reference to (2), this means reconstructing the value of the vector f_{ext}.

The more general instance of this problem can be easily shown to be unsolvable: if a system F_1 of two or more forces act simultaneously on the same phalanx of the hand, the net effect of that system of forces onto the robot mechanism is

[1]note that since the hypothesis of under-actuation, $n \leq s$

[2]the dimension M is equal to 3 times the number of contact points if rigid contact is assumed, or 6 times the number of contacts if soft contact is accounted for [21].

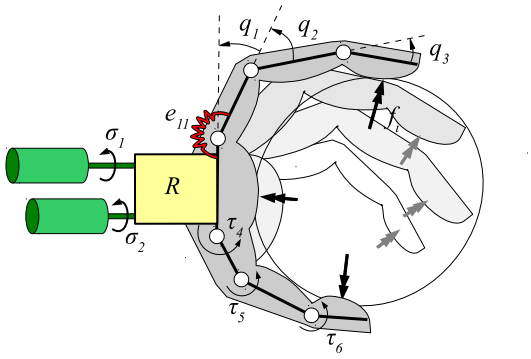

Fig. 2. Schematic of an under-actuated robotic hand with elastic return mechanisms grasping an object. Refer to the text for the definition of the symbols.

indistinguishable from another set F_2 with equal resulting wrench. Thus distinguish F_1 from F_2 is impossible, as any other system of forces with same resulting wrench.

So we will limit our problem to the reconstruction of the total wrench $f_{ext,i}$ acting on each phalanx. Note that in the case that a unique point contact is indeed acting to the phalanx, the knowledge of the total wrench $f_{ext,i}$ can be combined with knowledge of the phalanx geometry (e.g. with the algorithms proposed in [22]) yield also reconstruction of the contact point. Otherwise, in the hypothesis of a distribution of contact pressure, the same algorithms can be used to reconstruct a point on the convex closure of the surface in which the force of the wrench can be considered to be applied, called *centroid of contact* (see again [22] for more details).

Finally, in delineating the outlines of our problem we limit our analysis to planar fingers with pin joints orthogonal to the plane. This simplifying step will allow us an easier dissertation of a complex problem. Nevertheless, the results of our approach can still yield meaningful results in realistic use cases, being the planarity of fingers rather common among robot hands.

III. NAIVE SOLUTION

By evaluating Eq. (2) when $f_{\text{ext}} = 0$, we obtain the force balance along the synergistic closure

$$0 = R^T f - E(q^\star)\,, \tag{4}$$

where $q^\star \in \mathbb{R}^n$ is the hand free closure. Subtracting it from Eq. (2) leads to

$$J^T f_{\text{ext}} = -(E(q^\star) - E(q))\,. \tag{5}$$

This balance clearly relates the differences between actual and free closures q and $q^\star$ to the external wrenches $J^T f_{\text{ext}}$ through the elastic field E. For linear elastic fields this relation is further empathized in $J^T f_{\text{ext}} = -E\,(q - q^\star)$.

Ideally an estimator for the external forces can be obtained by expliciting f_{ext} as

$$f_{\text{ext}} = -J^{-T}(E(q) - E(q^\star))\,. \tag{6}$$

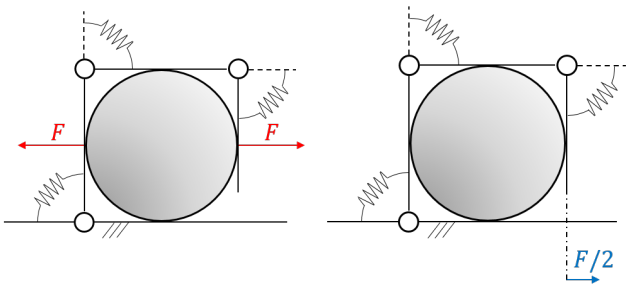

(a) Real Forces (b) Pseudoinverted Forces

Fig. 3. Even in a very simple grasp (a), to regress the interaction forces through pseudo-inversion generates incoherent results (b). The algorithm identifies just a force, exerted on the third phalanx outside the range of the finger.

This approach however present a main limitation: the Jacobian matrix $J(q)$ is in general not invertible. Indeed for a planar finger with no knowledge of contact points the Jacobian is the non-square matrix $J(q) \in \mathbb{R}^{n\times 3n}$, where n is the number of joints.

A straightforward method to solve this redundancy could rely on the use of Moore-Penrose pseudo-inversion $J^{+T}(q)$. Being the number of unknowns larger than the number of equations, this method would brings to a solution compatible with the system of equations. However there are at least two strong limitations to what the algorithm can do.

First, among all the possible solutions, pseudo-inversion takes the one of minimum norm. But there is a problem in defining norm for wrenches: being them composed by a mixture of forces and torques, they must be normalized with respect to some characteristic values. These values are in general arbitrary and in practice can be hard to find. Moreover the goodness of the solution has some amount of dependence on them, so it is not unique.

Second, the choice of minimizing the norm of the solution can imply considering solutions that are clearly non-compatible with the physical reality. To further clarify this point we report in Fig. 3 the example of a 3-DoF finger grasping a sphere. Each phalanx is consider of the same length L. The finger is in contact with the object in the middle point of each phalanx. As result of the grasping, two forces F are exerted on the medial and distal phalanges, as in Fig. 3(a). The corresponding external torque on the joints is $R^T f - E(q) = \begin{bmatrix}0 & -\frac{L}{2}F & -\frac{L}{2}F\end{bmatrix}^T$. By solving (6) through pseudo-inversion, i.e. as $J(q)^+(R^T f - E(q))$, the estimation in Fig. 3(b) results. Notice in particular how a pair of identical forces applied in the center of the phalanges is translated in one force applied on just one phalanx along a line that is not compatible with the phalanx geometry.

IV. PROPOSED ALGORITHM

As the previous section clearly showed, there are important motivations to avoid solving the redundancy of equation (5) with a simple pseudo-inverse. The most overwhelming is that the pseudo-inverse based solution leads to the reconstruction of forces that are manifestly not compatible with our insight of the hand-environment system and its physical constraints. This is why we propose to solve redundancy by incorporating this knowledge of the system in the form of a set of reasonable simplifying hypotheses that constrain the solution of the problem within the domain of physical sense.

A. Hypothesis $H1$: localized contact.

As it is clear in Fig. 3(b), the most manifest incoherence of the pseudo-inverse approach is the generation of solutions corresponding to forces applied on lines that do not intersect the geometry of the phalanges. This is inconsistent with any real system of contact forces applied to the phalanx body on its surface. So, to reduce the space of the possible solution, we start by including the constraint that forces can occur only in the phalanges and not outside them.

The most general form of the contact Jacobian J has a structure as in equation (3). To include constraint $H1$, given the frame attached to each phalanx, describe the set of points inside the i-th phalanx as an implicit function of two variables u_i, v_i as in

$$p_i = \begin{bmatrix} p_{x,i}(u_i, v_i) & p_{y,i}(u_i, v_i) \end{bmatrix}, \tag{7}$$

such that $u_i, v_i \in [0,1]$ (or other similar closed compact intervals). Then consider only the force component of each Jacobian but parametrized with respect to u_i, v_i. The full contact Jacobian would have a shape of the form

$$J_c^T = \left[J_1^T(u_1, v_1),\ J_2^T(u_2, v_2), \cdots\right], \tag{8}$$

Where the subscript c is for constrained. At this point our problem becomes

$$\begin{cases} J_c^T f_{\text{ext}} = -(E(q^\star) - E(q)) \\ u_i \in [0,1] \\ v_i \in [0,1] \end{cases} \tag{9}$$

Note that the space of the problem solution shrunk by n unconstrained variables (all the contact torques) but grew by $2n$ constrained variables and became non-linear. This can be considered as an inconvenience. To overcome this limitation, a stronger assumption can be substituted to $H1$, namely $H1^*$:

- Given that the geometry of the phalanges is in general small with respect to that of the full hand, assume that forces are applied exactly in the middle of each phalanx (see Fig. 5(a)).

As we will see in our application (sec. VI) this hypothesis is particularly reasonable due to the phalanges geometry and dimensions. Under this assumption the set of feasible u_i and v_i for each phalanx collapses to one point $u_i = u_{i*}, v_i = v_{i*}$. This leads to the new formulation of the problem as

$$J_{c^*}^T f_{\text{ext}} = -(E(q^\star) - E(q)), \tag{10}$$

where

$$J_{c^*}^T = \left[J_{1*}^T, J_{2*}^T, \cdots\right]. \tag{11}$$

and each $J_{i*}^T = J_i^T(u_{i*}, v_{i*})$. Note that now the new problem shrunk by the $2n$ variables u_i, v_i and become, once again, linear (J_{c*} is constant). The new problem is n variables smaller than the original 5 (each J_{i*}^T has one column less than the corresponding J_i^T). However $J_{c^*}^T$ is not square, thus no straightforward solution can still be found.

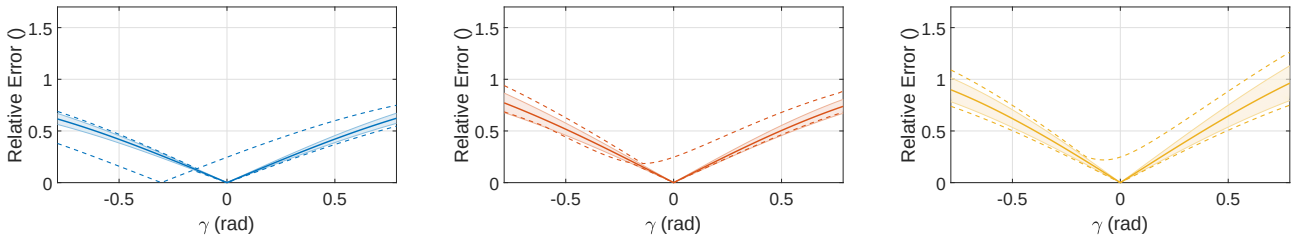

(a) Proximal (b) Medial (c) Distal

Fig. 4. Simulative results performed in the case of external forces non-orthogonal to the phalanx. We consider forces in $[0.25, 0.75]$N, exerted respectively on Proximal phalanx (a), Medial Phalanx (b), Distal Phalanx (c). γ is the angle that force has with its orthogonal. The line indicates the mean, the band contains all the simulated evolutions for $M = 0$. The dotted lines represent maximum and minimum performance also considering an external torque $M \in [-2, 2]$Nmm.

B. Hypothesis H2: friction cone compatibility.

Another constraint that will help containing the space of the possible solutions is that imposed by friction: assuming that the hand contact reached a steady state, the forces exchanged between the phalanges and the world should be compatible with the friction cone. This can be modeled in the most general case as a non-linear constraint involving the ratio between the different components of the contact wrenches represented on a reference frame defined with respect to the normal and tangent direction on the point of the contact. For example, if we indicate the normal to the phalanx surface on the contact points with $n_i(q)$, this changes the original problem in

$$\begin{cases} J^T f_{\text{ext}} = -(E(q^\star) - E(q)) \\ < f_{\text{ext},i}, n_i(q) > / ||f_{\text{ext},i}|| \geq \cos(\alpha_i) \,, \end{cases} \tag{12}$$

where α_i is the angle of static friction cone on the i-th contact, $< \cdot, \cdot >$ is the scalar product, and $||\cdot||$ is the euclidean norm.

Note that hypothesis $H2$ shrinks the space of the feasible solutions by adding n non-linear inequalities. Once again the non-linearity of the constraint can present difficulties during the solution phase, so we introduce a stronger version of hypothesis $H2$, justified by the domain of application of hands is for a large part defined by the task of grasping[3]. Hypothesis $H2^*$ is

- Given the typical contact condition of the hand on objects during grasping, we assume that forces are orthogonal to the contact surface of each phalanx.

$H2^*$ has the effect of collapsing the friction cone to a ray originating from the contact point and directed toward the phalanx. Combing $H2^*$ with $H1^*$ reduces problem (10) to

$$\begin{cases} J_{c^*}^T f_{\text{ext}} = -(E(q^\star) - E(q)) \\ f_{\text{ext},i} = n_i ||f_{\text{ext},i}|| \,. \end{cases} \tag{13}$$

Substituting $\lambda_i = ||f_{\text{ext},i}||$ the system becomes

$$\begin{cases} J_{c^*}^T N \lambda = -(E(q^\star) - E(q)) & (14) \\ \lambda_i \geq 0 \,, & (15) \end{cases}$$

[3]The robustness of the system to slight deviation from the assumptions $H1^*$ and $H2^*$ will be discussed in the following sections.

where

$$N = \begin{bmatrix} n_1(q) & 0 & \cdots & 0 \\ 0 & n_2(q) & \ddots & \vdots \\ \vdots & \ddots & \ddots & 0 \\ 0 & \cdots & 0 & n_n(q) \end{bmatrix} . \tag{16}$$

Note that now the matrix $J_{\text{r}} \triangleq J_{c^*}^T N$ is square, thus the problem becomes a linear square problem of size n with n linear inequality constraints added, expressed by (15).

If J_{r} is invertible, which we will assume, problem (14) can be solved as

$$\hat{\lambda} = J_{\text{r}}^{-T}(q)(E_{P,k}(q^\star) - E_{P,k}(q)) \,, \tag{17}$$

which leads to

$$\hat{f}_{\text{ext}} = N(q)\lambda = N(q) J_{\text{r}}^{-T}(q) \left(E_{P,k}(q^\star) - E_{P,k}(q)\right) . \tag{18}$$

Constraint (15) can be used to check the validity of the solution. To account for imprecision in the solution, coming from deviations from the hypotheses $H1^*$ and $H2^*$, we modify the algorithm in its final form by introducing the hypothesis of non-adhesive forces

$$\hat{f}_{\text{ext}} = N(q)[J_{\text{r}}^{-T}(q)(E_{P,k}(q^\star) - E_{P,k}(q))]^+ \,, \tag{19}$$

where $\hat{f}_{\text{ext}} \in \mathbb{R}^n$ is the estimation of contact forces, and $[\,\cdot\,]^+$ is the element-wise saturation to positive values.

V. SIMULATION RESULTS

To understand the limits of performance of the proposed algorithm, we test its behavior with respect to relaxations on the assumptions $H1^*$ and $H2^*$. The simulated system is a planar finger, with three phalanxes, actuated through a single motor

$$\begin{cases} J(q)^T f_{\text{ext}} & = R^T f - E(q) \\ \hat{f}_{\text{ext}} & = [J_{\text{r}}^{-T}(q)(E(q^\star) - E(q))]^+ . \end{cases} \tag{20}$$

We evaluate the reconstruction quality as the $2-$norm of the normalized difference between reconstructed external forces $\hat{f}_{\text{ext}}$ and the actual ones f_{ext}

$$\frac{||\hat{f}_{\text{ext}} - f_{\text{ext}}||}{||f_{\text{ext}}||} . \tag{21}$$

We consider here the $i-$th element of the external force as $f_{\text{ext},i} = \begin{bmatrix}1 & \sin(\gamma)\end{bmatrix}^T F_i$, see Fig. 6(a). By varying γ we set the distance of the force exerted from the orthogonality hypothesis. We consider here a quite large friction cone of $\gamma \in [-\frac{\pi}{4}, \frac{\pi}{4}]$. We simulate the system (20) for $f \in [25,75]$Nmm, $R_e = [10\ 10\ 10]$mm. The non linear model of the elastic field $E(q)$ is taken as the one of our hardware, that we present in the next sections, with $P = [0\ 0\ 0]$, $k = [0.5\ 0.5\ 0.5]\frac{\text{Nmm}}{\text{rad}}$, $R = [1\ 1\ 1]$mm. We consider three scenarios, in each one the force is applied on a single phalanx $F_i \in [0.25, 0.75]$N. We also consider a torque applied to the same phalanx $M_i \in [-2,2]$Nmm. Fig. 4 presents the resulting values of the cost index. The solid line indicates the mean performance, the band contains the simulated evolutions for $M_i = 0$. The dotted lines refer to the best and worst performance for a fixed γ. As expected, estimation error is null when the orthogonality hypothesis is verified, i.e. when $\gamma = 0$. The estimation error increases as the hypothesis is relaxed, i.e. for increasing values of $|\gamma|$. However, results show that for the considered range of parameters the relative error remains in the worst case under 0.5 by considering a maximum force inclination of $\gamma = 0.3$rad. Maximum mean errors are 0.6 for a force exerted on the proximal phalanx, 0.8 for a force exerted on the medial phalanx, and 1.0 for a force exerted on the distal phalanx.

VI. APPLICATION TO THE PISA/IIT SOFTHAND

To apply the proposed algorithm to Pisa/IIT SoftHand we must first derive the form of its reduced Jacobian and its potential field. Together with the elastic term we consider here also the effects of gravity.

A. Reduced Jacobian

Every finger of Pisa/IIT SoftHand (Fig. 5) is composed by a set of phalanges implementing a *CORE* type joint [23]. Abduction joints are neglected in this analysis. Fig. 6(a) shows the kinematic model of a single joint in rest and flexed position. A pure rolling constraint between the two phalanxes is modeled through a virtual link (dashed in figure), with no mass, with the two associated angles constrained to be equal.

Therefore the finger kinematics is obtained as 6R model with three equality constraints that reduce the total number of DoF to 3. The reduced Jacobian $J_r^T(q)$ is

$$J_r^T = \begin{bmatrix} a_{11} & a_{12} & a_{13} \\ 0 & a_{22} & a_{23} \\ 0 & 0 & a_{33} \end{bmatrix} \in \mathbb{R}^{3\times 3}, \tag{22}$$

with

$$\begin{cases} a_{11} &= D\cos(\frac{q_1}{2}) + L \\ a_{12} &= D[\cos(q_2 + \frac{q_1}{2}) + 2\cos(\frac{q_2}{2})] + L[1 + 2\cos(q_2)] \\ a_{13} &= D[\cos(q_2 + q_3 + \frac{q_1}{2}) + 2\cos(q_3 + \frac{q_2}{2}) + 2\cos(\frac{q_3}{2})] \\ & \quad + L[2\cos(q_2 + q_3) + 2\cos(q_3) + 1] \\ a_{22} &= D\cos(\frac{q_2}{2}) + L \\ a_{23} &= D[\cos(q_3 + \frac{q_2}{2})] + 2\cos(\frac{q_3}{2}) + L[2\cos(q_3) + 1] \\ a_{33} &= D\cos(\frac{q_3}{2}) + L, \end{cases} \tag{23}$$

where L is the link length, and D is the virtual link length (i.e. the diameter of the primitive circle of the two gears, see also Fig. 6(a)). q_i is the $i-th$ element of q. It is worth to notice that the algorithm is well posed since J_r^T is always invertible for $q_i > 0$, $L > 0$, $D > 0$.

B. Non Linear Spring Model

In the Pisa/IIT SoftHand the elastic force $E(q)$ is implemented through a set of elastic ligaments. Each element connects two consecutive phalanxes as in Fig. 6(b). Even if we consider each ligament as a linear spring, the overall compliance characteristic is non-linear due to the kinematics of the connection. Indeed the i-th spring displacement due to variations of q_i can be written as

$$\Delta l_i(q_i) = 2R_i[\cos(\frac{q_i}{2} + \beta_i) - \cos(\beta_i) + P_i], \tag{24}$$

where R_i is the envelope radius of the finger, β_i is the angle of the spring connection with respect to the horizontal, P_i is the pre-stretch of the elastic (i.e. its displacement when $q_i = 0$). Note that R_i and β_i are accurately known by design, P_i instead can vary from element to element, due to fabrication dispersion.

Being the spring energy for each joint $\frac{1}{2}k_i\Delta l_i^2$, where k_i is the i-th spring elastic constant we obtain, by derivation, the i-th component of the elastic field $E(q)$ as

$$4k_iR_i^2[\cos(\beta_i) - \cos(\beta_i + \frac{q_i}{2}) + P_i]\sin(\beta_i + \frac{q_i}{2})\tanh(k_s\frac{q_i}{2}), \tag{25}$$

where $\tanh(k_s\frac{q_i}{2})$ is heuristically added to take into account the effect of the joint limits. k_s is a suitable constant chosen as a trade-off between accuracy and smoothness (in the following we consider $k_s = 80$Nmm). It is worth noticing that a variation of k_i changes mostly the slope of the characteristic, while a variation of P_i adds an offset to the curve.

C. Gravity torque

In the case of availability of hand posture measurement also the compensation of gravity can be included as

$$G(q) = J^T(q)(\mathbf{R}(q) \otimes [1,1,1])\begin{bmatrix}F_{g1}^T & F_{g2}^T & F_{g2}^T\end{bmatrix}^T, \tag{26}$$

where $\otimes$ is the Kronecker product, $J(q)$ is the full Jacobian, $F_{gi} = [0\,,0\,,m_ig]^T$ is the weight force acting on link i defined by m_i, the mass of the $i-$th link and g, the gravity acceleration. $\mathbf{R}(q)$ is a rotation matrix opportunely parametrized by a set of three angles included in $q \in \mathbb{R}^9$. Neither $J(q)$, nor $\mathbf{R}(q)$, are explicitly reported here for the sake of space. Note that all the elements appearing in $G(q)$ are already considered known by design, and so they can be directly compensated during the calibration procedure.

VII. EXPERIMENTAL RESULTS

A. Experimental Setup

To experimentally validate the proposed method, we developed a gripper adopting two fingers of Pisa/IIT SoftHand, derived from the one described in [24]. The gripper design will be made openly available as part of the NMMI platform

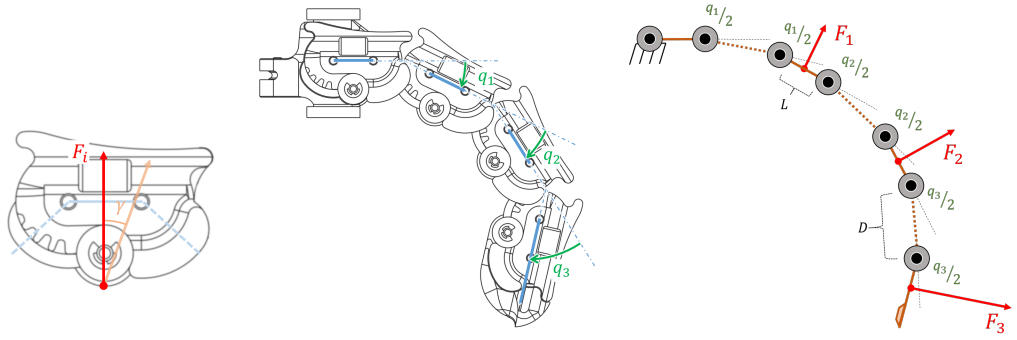

(a) (b) (c)

Fig. 5. Pisa/IIT SoftHand finger with main variables underlined. (a) shows the contact force F_i point of application. γ is the angle of a generic force applied in the same contact point w.r.t. F_i. (b) shows the whole finger structure. q_i is the angle between i-th and previous phalanxes. (c) presents the kinematic model of the finger, a 6R serial robot, with 3 equality constraints. Also the contact forces F_1, F_2, F_3 are reported.

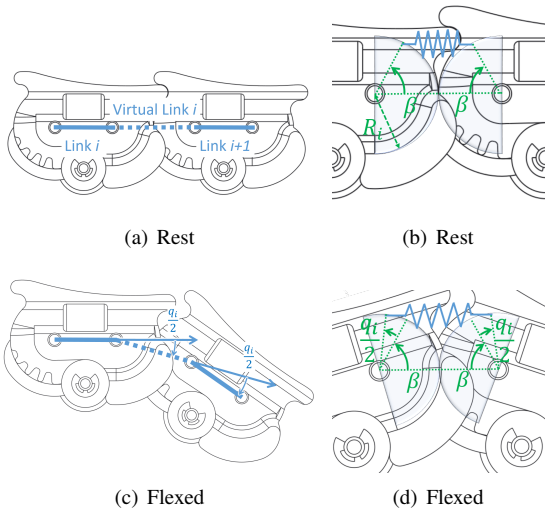

(a) Rest (b) Rest

(c) Flexed (d) Flexed

Fig. 6. Interphalangeal joint, a realization of CORE joint. Due to the pure revolution constraint between the two phalanxes we model a single joint as an RR arm, with a mass-less intermediate link, and an equality constraint between the two angles. The interphalangeal spring system is represented in rest (a) and flexed (b) positions. q_i is the joint angle, β is the angle of the spring connection with respect to the horizontal, R_i is the envelope radium

[8]. On each phalanx there is an IMU and a normal force sensor. In this work we will use the force sensors as ground truth to compare the results of the proposed algorithm. The IMUs readings are used to reconstruct the hand posture.

B. Algorithm

Fig. 7(b) shows a scheme of the implemented algorithm, with its two inputs: the measure of the motor current i, and the measure of accelerations a and angular velocities ω from the IMUs. We estimate the motor torque from the current by considering the simple static relation $f = \alpha_M i$, where α_M is the product of motor torque-current constant and the gear ratio. Joint angles $q \in \mathbb{R}^6$ are estimated from acceleration a and angular velocity ω, coming from IMU measurements, through an implementation of passive complementary Mahony filter [25]. The particularity of this filter is to not directly integrate accelerations a but to use them to measure the gravity acceleration, and thus regress the rotation w.r.t. to the local vertical. The time discrete dynamics of the filter is

$$A^i_n = A^i_{n-1} + A^i_{n-1}(\delta_n + \Omega)\Delta t\,, \tag{27}$$

where A^i_{n-1} is the rotation matrix at the step $n-1$ from the $i-$th IMU frame to a fixed inertial inertial one. Ω is the skew matrix of the angular velocity ω at the step n, and δ_n is a correction factor which depends linearly from the cross product between the acceleration a in IMU frame and the gravity g considering the rotation A_{n-1}. Finally Δt is the time between two steps. The $i-$th element of q is evaluated by looking to the rotation matrix that maps A^{i-1}_n into A^i_n. See [24] for more details. The force and joint angle estimations f and q are then used to estimate the contact forces $\hat{f}_{\text{ext}}$, according to the proposed algorithm.

Model parameters are all known by design, except to P, k which were estimated by solving

$$\arg\min_{P,k} \sum_{i=1}^{m} ||R^T \tilde{f}^i - E_{P,k}(\tilde{q}^i)||^2\,, \tag{28}$$

where $\tilde{f}^i$ and $\tilde{q}^i$, for $i \in \{1 \dots m\}$ are m measures acquired from a single closure (see Fig. 8). The problem is non-convex, so we solved it by an exhaustive evaluation of the cost function in the value of an opportune lattice of the interval $[0,30]\frac{\text{Nmm}}{\text{rad}} \times [0,30]\frac{\text{Nmm}}{\text{rad}} \times [0,30]\frac{\text{Nmm}}{\text{rad}}$ for the stiffness k and $[0,3] \times [0,3] \times [0,3]$ for the pretension P. The result is refined through a classic gradient-descent algorithm, implemented in MatLab function `FminCon`.

C. Results

The following parameters resulted from the identification procedure: $k = \begin{bmatrix}0.23 & 0.34 & 0.26\end{bmatrix}^T \frac{\text{Nmm}}{\text{rad}}$, $P = \begin{bmatrix}0.72 & 0.51 & 0.65\end{bmatrix}^T$. Fig. 9 shows the comparison between joint torque estimated through elastic and gravitational model $E_{P,k}(q) + G(q)$ and the current used by the motor $R^T \alpha_M i$. The two trends match with a good accuracy, with a discrepancy in the first 15s probably due to the presence of un-modeled friction effects. This translates in errors of less

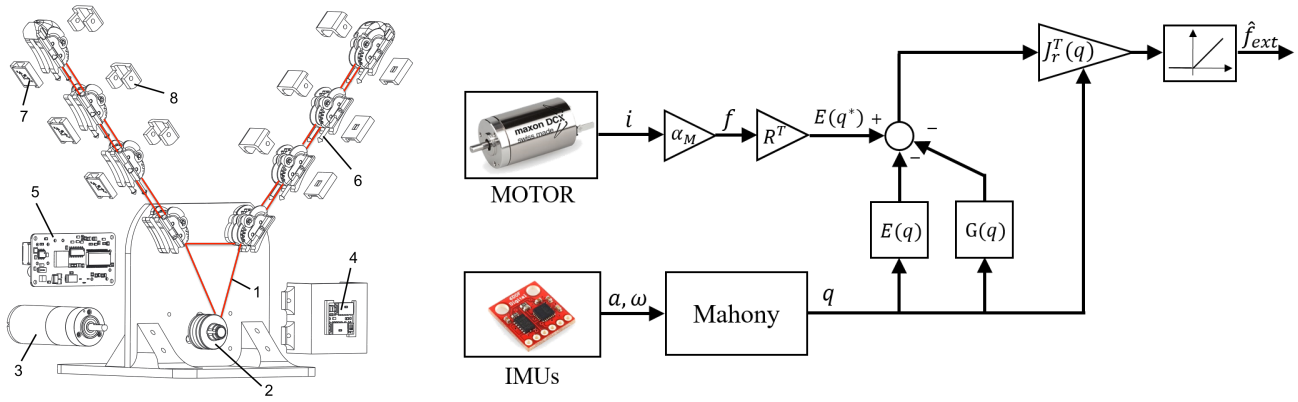

(a) Testbed (b) Scheme

Fig. 7. To evaluating the proposed algorithm in a realistic condition we designed the experimental setup in (a). It is a two-fingered planar gripper with 6-DoF, actuated by the motor (3) through the single tendon (1) connected to the pulley (2). The motor angle is acquired through the encoder (4). Each phalanx is equipped with an IMU (7) providing measures of angular velocity and acceleration, and a normal force sensor (8) as benchmarking. The low level control is implemented in the custom board (5). (b) presents the scheme of the employed algorithm, combining the one proposed in this work with a Mahony fitler for the estimation of joint angles and with a simple static estimator of motor generalized force.

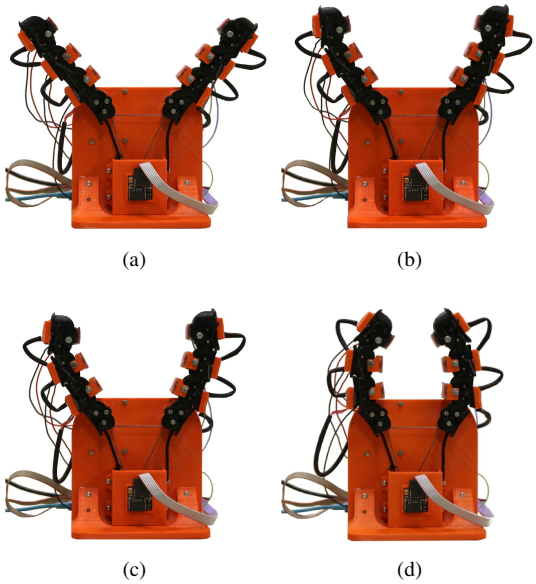

(a) (b) (c) (d)

Fig. 8. Photo-sequence of the gripper free-closure.

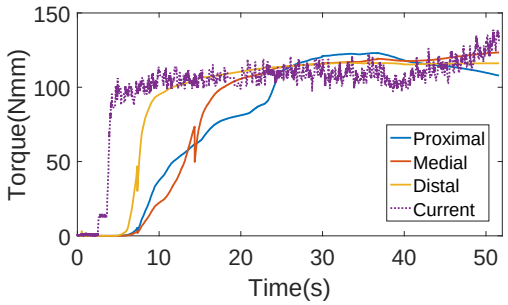

Fig. 9. Comparison between joint torque estimated through elastic and gravitational model $E_{P,k}(q)+G(q)$ and the current used by the motor $R^T\,\alpha_M\,i$ for the left finger of the gripper.

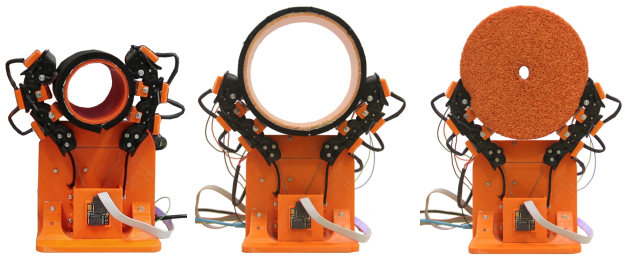

(a) (b) (c)

Fig. 10. Final grasping configuration for the three objects considered in the experiments.

than 0.1Nmm in estimating forces during the free closure of the gripper.

The ability of the algorithm in estimating interaction forces is evaluated through the grasping of three cylinders of different radii and softness: 30mm rigid, 60mm rigid, 60mm soft. The two rigid objects are covered with a layer of neoprene, to increase the dimension of friction cone to further reduce the similarity with the imposed hypothesis.

Fig. 10 shows the final posture of the grasp for the three objects. Fig. 11 shows the evolution of both estimated and measured forces. In all the three cases the algorithm successfully locates phalanges which are in contact. A good resemblance is present between force trends and magnitude individuated by the algorithm and measured by the sensors.

VIII. CONCLUSIONS

In this work we proposed an algorithm to estimate interaction forces in an under-actuated robotic hand. To solve analytically the problem we formulated reasonable hypotheses on the nature of such forces. The algorithm was then explicitly derived for a finger of Pisa/IIT SoftHand, and experimentally tested. Future work will be devoted to include in the algorithm compensatory terms taking in account neglected effects, and to test the algorithm effectiveness in

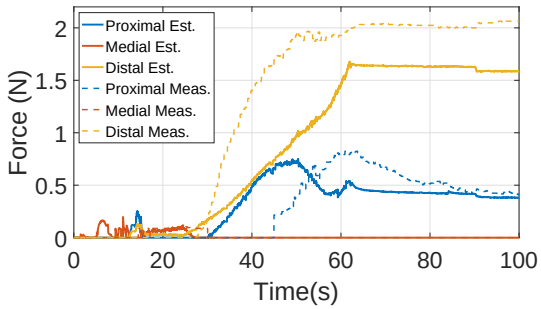

(a) Large Cylinder

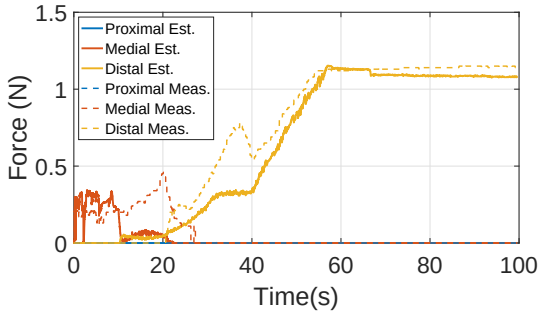

(b) Sponge

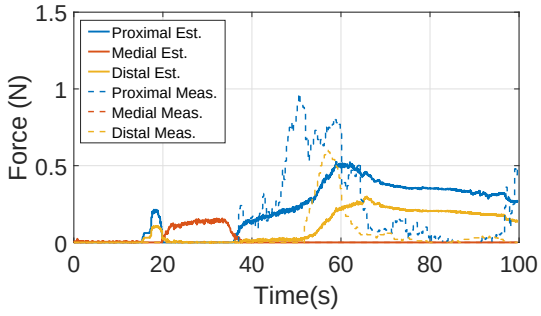

(c) Small Cylinder

Fig. 11. Measured and estimated interaction forces for the left finger of the gripper during the considered experiments. Forces estimated by the algorithm present same trend and magnitude of the measured ones, also allowing to correctly detect the phalanx in which the contact occurs

different experimental setups.

ACKNOWLEDGMENTS

The authors warmly thank Emanuele Luberto, Francesco Bufalo, Davide Fabbrioni, Lorenzo Tiberi, Alberto Brando, Andrea di Basco and Fabio Bonomo for their valuable help in the realization of the experimental prototype.

REFERENCES

[1] M. Grebenstein, A. Albu-Schäffer, T. Bahls, M. Chalon, O. Eiberger, W. Friedl, R. Gruber, S. Haddadin, U. Hagn, R. Haslinger *et al.*, "The dlr hand arm system," in *Robotics and Automation (ICRA), 2011 IEEE International Conference on*. IEEE, 2011, pp. 3175–3182.

[2] L. U. Odhner, L. P. Jentoft, M. R. Claffee, N. Corson, Y. Tenzer, R. R. Ma, M. Buehler, R. Kohout, R. D. Howe, and A. M. Dollar, "A compliant, underactuated hand for robust manipulation," *The International Journal of Robotics Research*, vol. 33, no. 5, pp. 736–752, 2014.

[3] R. Deimel and O. Brock, "A novel type of compliant and underactuated robotic hand for dexterous grasping," *The International Journal of Robotics Research*, p. 0278364915592961, 2015.

[4] A. Albu-Schaffer, O. Eiberger, M. Grebenstein, S. Haddadin, C. Ott, T. Wimbock, S. Wolf, and G. Hirzinger, "Soft robotics," *IEEE Robotics & Automation Magazine*, vol. 15, no. 3, pp. 20–30, 2008.

[5] L. Birglen, C. M. Gosselin, and T. Laliberté, *Underactuated robotic hands*. Springer, 2008, vol. 40.

[6] M. G. Catalano, G. Grioli, E. Farnioli, A. Serio, C. Piazza, and A. Bicchi, "Adaptive synergies for the design and control of the pisa/iit softhand," *The International Journal of Robotics Research*, vol. 33, no. 5, pp. 768–782, 2014.

[7] C. Della Santina, G. Grioli, M. Catalano, A. Brando, and A. Bicchi, "Dexterity augmentation on a synergistic hand: The pisa/iit softhand+," in *Humanoid Robots (Humanoids), 2015 IEEE-RAS 15th International Conference on*. IEEE, 2015, pp. 497–503.

[8] C. Della Santina, C. Piazza, G. M. Gasparri, M. Bonilla, M. G. Catalano, G. Grioli, M. Garabini, and A. Bicchi, "The quest for natural machine motion: An open platform to fast-prototyping articulated soft robots," *IEEE Robotics & Automation Magazine*, 2017.

[9] A. Bicchi, M. Gabiccini, and M. Santello, "Modelling natural and artificial hands with synergies," *Philosophical Transactions of the Royal Society B: Biological Sciences*, vol. 366, no. 1581, pp. 3153–3161, 2011.

[10] M. Santello, M. Flanders, and J. F. Soechting, "Postural hand synergies for tool use," *The Journal of Neuroscience*, vol. 18, no. 23, pp. 10 105–10 115, 1998.

[11] M. Bonilla, E. Farnioli, C. Piazza, M. Catalano, G. Grioli, M. Garabini, M. Gabiccini, and A. Bicchi, "Grasping with soft hands," in *2014 IEEE-RAS International Conference on Humanoid Robots*. IEEE, 2014, pp. 581–587.

[12] R. Deimel, C. Eppner, J. Álvarez-Ruiz, M. Maertens, and O. Brock, "Exploitation of environmental constraints in human and robotic grasping," in *Robotics Research*. Springer, 2016, pp. 393–409.

[13] L. P. Jentoft and R. D. Howe, "Determining object geometry with compliance and simple sensors," 2011.

[14] G. S. Koonjul, G. J. Zeglin, and N. S. Pollard, "Measuring contact points from displacements with a compliant, articulated robot hand," in *Robotics and Automation (ICRA), 2011 IEEE International Conference on*. IEEE, 2011, pp. 489–495.

[15] B. Belzile and L. Birglen, "Stiffness analysis of underactuated fingers and its application to proprioceptive tactile sensing," *IEEE/ASME Transactions on Mechatronics*, vol. 21, no. 6, pp. 2672–2681, 2016.

[16] Z. Kappassov, J.-A. Corrales, and V. Perdereau, "Tactile sensing in dexterous robot handsreview," *Robotics and Autonomous Systems*, vol. 74, pp. 195–220, 2015.

[17] T.-H. Pham, A. Kheddar, A. Qammaz, and A. A. Argyros, "Towards force sensing from vision: Observing hand-object interactions to infer manipulation forces," in *Proceedings of the IEEE Conference on Computer Vision and Pattern Recognition*, 2015, pp. 2810–2819.

[18] A. I. Aviles, A. Marban, P. Sobrevilla, J. Fernandez, and A. Casals, "A recurrent neural network approach for 3d vision-based force estimation," in *2014 4th International Conference on Image Processing Theory, Tools and Applications (IPTA)*. IEEE, 2014, pp. 1–6.

[19] A. De Luca and R. Mattone, "Sensorless robot collision detection and hybrid force/motion control," in *Proceedings of the 2005 IEEE international conference on robotics and automation*. IEEE, 2005, pp. 999–1004.

[20] L. Birglen, T. Laliberté, and C. M. Gosselin, *Underactuated robotic hands*. Springer, 2007, vol. 40.

[21] A. Bicchi and V. Kumar, "Robotic grasping and contact: A review," in *Robotics and Automation, 2000. Proceedings. ICRA'00. IEEE International Conference on*, vol. 1. IEEE, 2000, pp. 348–353.

[22] A. Bicchi, J. K. Salisbury, and D. L. Brock, "Contact sensing from force measurements," *The International Journal of Robotics Research*, vol. 12, no. 3, pp. 249–262, 1993.

[23] J. R. Cannon and L. L. Howell, "A compliant contact-aided revolute joint," *Mechanism and Machine Theory*, vol. 40, no. 11, pp. 1273–1293, 2005.

[24] G. Santaera, E. Luberto, A. Serio, M. Gabiccini, and A. Bicchi, "Low-cost, fast and accurate reconstruction of robotic and human postures via imu measurements," in *2015 IEEE International Conference on Robotics and Automation (ICRA)*. IEEE, 2015, pp. 2728–2735.

[25] R. Mahony, T. Hamel, and J.-M. Pflimlin, "Nonlinear complementary filters on the special orthogonal group," *IEEE Transactions on automatic control*, vol. 53, no. 5, pp. 1203–1218, 2008.